Research Paper

Cytochalasin H Inhibits Angiogenesis *via* the Suppression of HIF-1α Protein Accumulation and VEGF Expression through PI3K/AKT/P70S6K and ERK1/2 Signaling Pathways in Non-Small Cell Lung Cancer Cells

Yuefan Ma[1,2]*, Zihan Xiu[1,2]*, Zhiyuan Zhou[1,2], Bingyu Huang[1,2], Jiao Liu[1,2], Xiaofeng Wu[1,2], Sanzhong Li[1,2], Xudong Tang [1,2,3,4]✉

1. Collaborative innovation center for antitumor active substance research and development, Guangdong Medical University, Zhanjiang 524023, P.R. China
2. Institute of Biochemistry and Molecular Biology, Guangdong Medical University, Zhanjiang 524023, P.R. China
3. Guangdong Key Laboratory for Research and Development of Natural Drugs, Guangdong Medical University, Zhanjiang 524023, P.R. China
4. Guangdong Provincial Key Laboratory of Medical Molecular Diagnostics, Guangdong Medical University, Dongguan 523808, P.R. China.

* These authors contribute equally to this work.

✉ Corresponding author: Xudong Tang, MD, PhD, Collaborative innovation center for antitumor active substance research and development, Guangdong Medical University, 2 Wenming Donglu, Xiashan, Zhanjiang, Guangdong 524023, P.R. China. Phone: 86-759-2388581, Fax: 86-759-2284104, E-mail: tangxudong2599@126.com, txd@gdmu.edu.cn.

Abstract

Our previous study has demonstrated that cytochalasin H (CyH) isolated from mangrove-derived endophytic fungus induces apoptosis and inhibits migration in A549 non-small cell lung cancer (NSCLC) cells. In this study, we further explored the effect of CyH on angiogenesis in NSCLC cells and the underlying molecular mechanisms. A549 and H460 NSCLC cells were treated with different concentrations of CyH for 24 h. The effects of CyH on NSCLC angiogenesis *in vitro* and *in vivo* were investigated. Hypoxia inducible factor-1α (HIF-1α) and vascular endothelial growth factor (VEGF) expression in xenografted NSCLC of nude mice was analyzed by immunohistochemistry. ELISA was used to analyze the concentration of VEGF in the conditioned media derived from treated and untreated NSCLC cells. Western blot was performed to detect the levels of HIF-1α, p-AKT, p-P70S6K, and p-ERK1/2 proteins, and RT-qPCR was used to determine the levels of HIF-1α and VEGF mRNA in A549 and H460 cells. Our results showed that CyH significantly inhibited angiogenesis *in vitro* and *in vivo*, and suppressed the hemoglobin content and HIF-1α and VEGF protein expression in xenografted NSCLC tissues of nude mice. Meanwhile, CyH inhibited the secretion of VEGF protein and the expression of HIF-1α protein in A549 and H460 cells. Moreover, CyH had a significant inhibitory effect on VEGF mRNA expression but had no effect on HIF-1α mRNA expression, and CyH inhibited HIF-1α protein expression by promoting the degradation of HIF-1α protein in A549 and H460 cells. Additionally, CyH dramatically inhibited AKT, P70S6K, and ERK1/2 activation in A549 and H460 cells. Taken together, our results suggest that CyH can inhibit NSCLC angiogenesis by the suppression of HIF-1α protein accumulation and VEGF expression through PI3K/AKT/P70S6K and ERK1/2 signaling pathways.

Key words: cytochalasin H (CyH), angiogenesis, hypoxia inducible factor-1α (HIF-1α), vascular endothelial growth factor (VEGF), PI3K/AKT/P70S6K, ERK1/2, non-small cell lung cancer (NSCLC), mangrove

Introduction

Lung cancer is the leading cause of cancer-related deaths in both men and women [1–4]. Non-small cell lung cancer (NSCLC) accounts for about 85% of lung cancers [5]. In spite of the introduction of modern therapeutic interventions such as chemotherapy, radiotherapy, and surgical

resection , the 5-year survival rate for all stages of NSCLC is quite poor [6–9]. Therefore, it is important that we explore novel drugs that show stronger efficacy along with robust safety profiles for the prevention and treatment of NSCLC.

Angiogenesis plays a major role in the development, progression, and metastatic spread of solid tumors *via* mediating proliferation, migration, and invasion of endothelial cells [10, 11] with the activation of several signaling molecules, such as extracellular signal-regulated kinase (ERK) and AKT [12–14]. Hypoxia inducible factor-1α (HIF-1α), a downstream target of PI3K, plays a key role in promoting cancer angiogenesis by regulating the expression of numerous factors [15]. HIF-1α is overexpressed in solid cancer cells including lung cancer [16], but it does not exist in most normal tissue [16]. It is clear that HIF-1α regulates vascular endothelial growth factor (VEGF) protein synthesis, one of the most potent and specific pro-angiogenic factor [17], through PI3K/AKT pathway [18]. VEGF plays a critical role in tumor growth and metastasis [19–21]. Accumulating evidence suggests that the inhibition of angiogenesis should become an important strategy for the treatment of solid tumors, including lung cancer [22–24].

Mangrove-derived endophytic fungi have been regarded as a rich source of structurally unique and biologically potent secondary metabolites, which have become interesting and significant resources for drug discovery. In our previous study, we have isolated cytochalasin H (CyH), a kind of cytochalasins, from the metabolites of endophytic fungus *Phomopsis liquidambari* derived from a type of mangrove plant in Zhanjiang, China, and demonstrated that CyH induced apoptosis and inhibited migration in A549 NSCLC cells [25]. CyH has been reported to inhibit angiogenesis and tumor growth [26, 27]. However, the effect of CyH on NSCLC angiogenesis remains unclear.

In the present study, we observed the effect of CyH on angiogenesis in A549 and H460 NSCLC cells. To the best of our knowledge, we found for the first time that CyH inhibited angiogenesis through the inhibition of HIF-1α protein accumulation, VEGF expression *via* PI3K/AKT/P70S6K and ERK1/2 signaling pathways in A549 and H460 cells. These findings suggest that CyH may be developed into a potential drug for anti-angiogenesis of NSCLC.

Materials and methods

Drug and reagents

CyH was dissolved in 0.1% dimethyl sulfoxide (DMSO) at a concentration of 1 mM, and was then diluted in cell culture medium according to experimental requirements. *In vitro* angiogenesis assay kit (ECM625) was obtained from Millipore (Temecula, CA, USA). BD Matrigel™ Basement Membrane Matrix High Concentration (354248) was obtained from BD Biosciences (Bedford, MA, USA). Human VEGF ELISA kit (cat. no. EK0539) was from Wuhan Boster Bio-engineering Limited Company (Wuhan, China). HiCN hemoglobin detection kit was from Shanghai Rongsheng Biotech Co., Ltd. (Shanghai, China). Mouse anti-human HIF-1α antibody (1:1000 dilution; cat. no. 610959) was purchased from BD Transduction Laboratories (San Diego, CA, USA). Rabbit anti-human AKT (Ser473, 1:1000 dilution; cat. no. 4685), rabbit anti-human phosphorylated AKT (p-AKT, Ser473, 1:1000 dilution; cat. no. 4060), rabbit anti-human P70S6K (1:1000 dilution; cat. no. 2708), rabbit anti-human phosphorylated P70S6K (p-P70S6K, 1:1000 dilution; cat. no. 9204), and rabbit anti-human ERK1/2 (Thr202/ Tyr204, 1:1000 dilution; cat. no. 9107) primary antibodies were purchased from Cell Signaling Technology (Danvers, MA, USA). Phosphorylated ERK1/2 (p-ERK1/2, Thr202/Tyr204, 1:1000 dilution; cat. no. AF1891) and goat anti-rabbit β-actin primary antibodies (1:1000 dilution; cat. no. AA128-1) were purchased from Beyotime Institute of Biotechnology (Shanghai, China). Rabbit anti-human VEGF polyclonal primary antibody (1:1000 dilution; cat. no. AF11182863) was purchased from Beijing Biosynthesis Biotechnology Co., Ltd (Beijing, China). Goat-anti mouse-HRP (1:2000 dilution; cat. no. 707 6S) and goat-anti rabbit-HRP (1:2000 dilution; cat. no. 7074S) secondary antibodies were purchased from Cell Signaling Technology (Danvers, MA, USA). One Step SYBR® PrimeScript® RT-PCR (No. DRR086A) was obtained from TaKaRa Biotechnology Co., Ltd. (Dalian, China). Gibco® RPMI-1640 medium was purchased from Thermo Fisher Scientific, Inc. (Waltham, MA, USA).

Cells and animals

Human NSCLC cell line A549 and human umbilical vein endothelial cells (HUVECs) were purchased from the American Type Culture Collection (ATCC; Rockville, MD, USA). Human NSCLC cell line H460 was obtained from the Chinese Academy of Sciences Cell Bank of Type Culture Collection (Shanghai, China). A549 and H460 cells were cultured in RPMI-1640 medium containing 10% fetal bovine serum (FBS), 100 U/ml of penicillin and 100 µg/ml streptomycin. HUVEC cells were cultured in DMEM medium supplemented with 10% fetal bovine serum (FBS), 100 U/ml of penicillin and 100 µg/ml streptomycin. All cells were cultured in a 5% CO_2 incubator at 37 °C. Cells in the logarithmic phase

of growth were used in the experiment.

6~8-week-old male BALB/c nude mice with 20~22 g weight were purchased from Beijing Vital River Laboratory Animal Technology Co., Ltd (Beijing, China). The animals were housed in an air--conditioned room at 23~25 °C. All experiments with animals were undertaken in accordance with the institution guidelines of the Institutional Animal Care and Use Committee of Guangdong Medical University.

Western blot analysis

The method was as described previously [28–30]. Briefly, A549 and H460 cells were treated with CyH (0, 6.25, 12.5, and 25 µM) for 24 h. The cells were washed with cold PBS, collected, and lysed on ice with RIPA lysis buffer containing protease inhibitors for 1 h, then centrifuged at 12,000 rpm for 10 min. Protein concentration was detected by the BCA protein assay. Afterwards, 100 µg of protein samples were separated on 10% SDS-PAGE and transferred to a PVDF membrane (Millipore, Billerica, MA, USA). The membrane was blocked with 5% non-fat milk or TBS for 2 h at room temperature, and incubation overnight at 4°C with various primary antibodies against HIF- 1α, AKT, p-AKT, P70S6K, p-P70S6K, ERK1/2, or p-ERK1/2, followed by incubation with HRP-conjugated secondary antibodies (1:2000). Target proteins were detected by ECL reagents and measured using ImageJ software (National Institutes of Health, Bethesda, MD, USA).

RT-qPCR

The method was as described previously [28–30]. Briefly, A549 and H460 cells were treated with CyH (0, 6.25, 12.5, and 25 µM) for 24 h. Total RNA from the cells was extracted with TRIZOL® Reagent (Invitrogen; Thermo Fisher Scientifc, Inc.) according to the manufacturer's protocol. RT-qPCR analysis of HIF-1α, VEGF, and β-actin mRNA levels was performed using One Step SYBR® PrimeScript® RT-PCR (TaKaRa, China). The specific primers synthesized by Sangon Biotech (Shanghai, China) were as follows: HIF-1α forwards 5′-TCTGGGTTGAAACTCAAGCAACTG-3′ and reverse 5′-CAACCGGTTTAAGGACACATTCTG -3′ [Genbank: NM_001243084.1]; VEGF forwards 5′-T GCTTCTGAGTTGCCCAGGA-3′ and reverse 5′-TGG TTTCAATGGTGTGAGGACATAG-3′ [Genbank:NM_ 001287044.1]; β-actin forwards 5′-TCATGAAGTGTG ACGTGGACATCCGT-3′ and reverse 5′-CCTAGAAG CATTTGCGGTGGACGATG-3′ [Genbank:NM_00110 1.4]. The cycling conditions were as follows: 42 °C for 5 min, 95 °C for 10 s, followed by 40 cycles at 95 °C for 5 s, and 60 °C for 31 s. Target gene mRNA levels were normalized to β-actin by using $2^{-\Delta\Delta Ct}$.

Enzyme linked immunosorbent assay (ELSIA)

The method was as described previously [28–30]. Briefly, 5×10^5 cells were plated in each well of a 6-well plate and were treated with various concentrations (0, 6.25, 12.5, and 25 µM) of CyH. After 24 h, the supernatant was collected and centrifuged at 1,000 rpm for 5 min. A human VEGF ELSIA kit was used to analyze VEGF concentration in the conditional media of A549 and H460 cells according to the manufacturer's protocols. The experiment was repeated at least three times.

In vitro angiogenesis assay

The method was as described previously [30]. Briefly, Matrigel was thawed at 4 °C overnight. Next day, the thawed Matrigel was placed in a 96-well plate and polymerized for 30 min at 37 °C. HUVECs (5×10^3/well) were plated onto the Matrigel layer in the culture medium containing various concentrations (0, 0.78, 1.56, 3.13, and 6.25 µM) of CyH. After incubation for 6~8 h, the tube formation was visualized and imaged under a phase-contrast microscope (Nikon, Tokyo, Japan). The total tube length in three random view-fields per well was measured by Scion Image software, and average value was calculated.

In vivo angiogenesis assay

The method was as described previously [30]. Briefly, A549 and H460 cells were treated with different concentrations (0, 6.25, 12.5, and 25 µM) of CyH. After 24 h, the cells were re-suspended in media at 8.0×10^6 cells/mL, and 0.25 mL (2×10^6 cells) of cell suspension was mixed with the same volume of BD Matrigel Matrix (0.25 mL) on ice. Then, the mixture was injected into axillary lateral subcutaneous of nude mice. Animals were euthanized and the Matrigel plugs were excised after 10 days, with half of each Matrigel plug fixed with 10 % neutral formalin for immunohistochemical staining, and the other half for the determination of hemoglobin content. The hemoglobin concentration of samples was determined spectrophotometrically by measuring absorbance at 540 nm.

Immunohistochemistry

Immunohistochemical staining was performed to analyze HIF-1α and VEGF expression in Matrigel plugs. The method was as described previously [30]. Briefly, 4-µm tissue sections was fixed and paraffin-embedded. All sections were then deparaffinized in xylene, rehydrated through serial dilutions of alcohol, and washed with PBS (pH 7.2). The sections were respectively incubated with anti-HIF-1α (1:100) and anti-VEGF (1:100) primary antibodies overnight at

4°C, followed by incubation with HRP-conjugated secondary antibody for 1 h at room temperature. Staining was detected with 3,3'-diaminobenzidine tetrahydrochloride (DAB) and observed under a light microscope (Nikon, Tokyo, Japan).

Statistical analysis

All data are showed as mean ± standard deviation. One-way ANOVA assay was performed for data analysis using SPSS 16.0 statistical software (SPSS, Inc., Chicago, IL, USA). $P < 0.05$ was indicative of a statistically significant difference.

Results

CyH inhibited NSCLC angiogenesis *in vitro*

To explore the effect of CyH on angiogenesis of NSCLC *in vitro*, the Matrigel tube formation assay was used to evaluate the capillary tube formation of HUVECs stimulated by the conditioned media derived from CyH-treated A549 or H460 cells. As expected, the conditioned media in the solvent control group significantly stimulated microtubule formation of HUVECs **(Figure 1A and 1B, lane 2)**. After A549 and H460 cells were treated with different concentrations (0, 0.78, 1.56, 3.13, and 6.25 μM) of CyH, microtubule formation of HUVECs was inhibited **(Figure 1A and 1B)**, and the length of the total tube was significantly shortened ($P < 0.05$, **Figure 1C and 1D)**. The inhibitory effect was enhanced with the increase of CyH concentration ($P < 0.05$, **Figure 1)**. Taken together, our data demonstrated that CyH inhibited NSCLC angiogenesis *in vitro*.

CyH inhibited angiogenesis *in vivo* and the expression of HIF-1α and VEGF in A549 and H460 xenografted tumor models

Considering that CyH dramatically inhibited angiogenesis *in vitro*, we further explored the effect of CyH on NSCLC angiogenesis *in vivo* by Matrigel plug assays in BALB/c nude mice. Our results showed that the solvent controls exhibited obvious angiogenesis and showed much higher hemoglobin levels **(Figure 2A and 2B, lane 2)**. After A549 and H460 cells were treated with CyH (6.25, 12.5, and 25 μM), the angiogenesis was significantly reduced **(Figure 2A and 2B)**. These results were further confirmed by the quantification of the hemoglobin content in tumor xengrafts ($P < 0.01$, **Figure 2C and 2D)**. We then examined the histology and HIF-1α and VEGF protein expression in tumor xenografts by H&E staining and immunohistochemistry, respectively. As shown in **Figure 2E and 2F**, the location of immunoreactivity to HIF-1α and VEGF was in nuclei and cytoplasm, respectively. Moreover, CyH significantly suppressed HIF-1α and VEGF protein expression **(Figure 2E and 2F)**. Taken together, these results indicated that CyH obviously inhibited the *in vivo* angiogenesis of NSCLC.
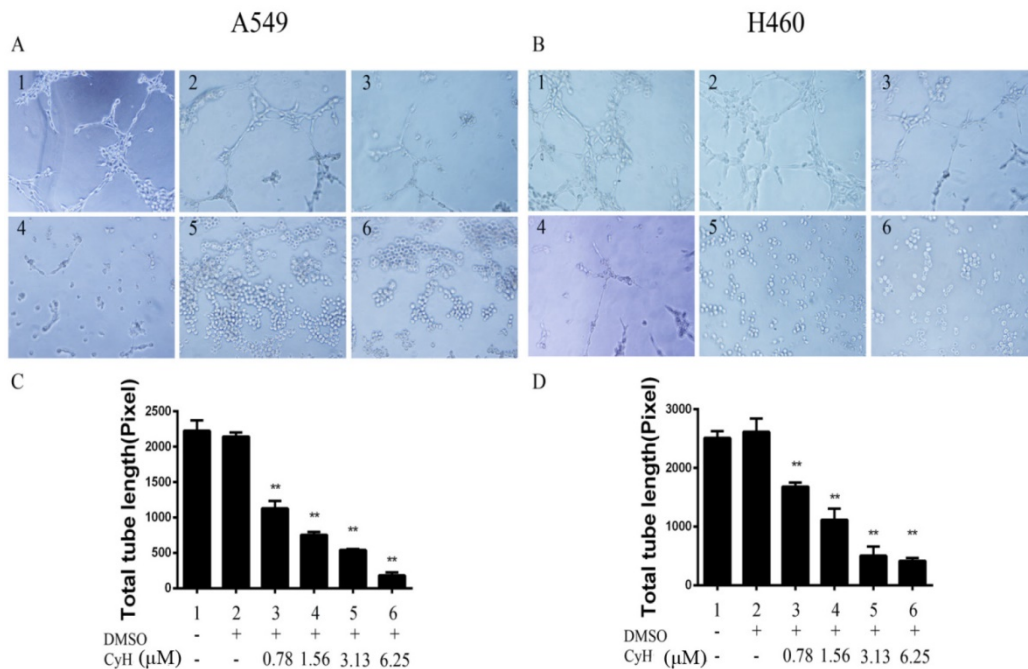

Figure 1. CyH inhibited the capillary tube formation *in vitro*. HUVECs (5×10^3 /well) were seeded onto the surface of 96-well cell culture plates pre-coated with polymerized ECMatrix™ and then incubated at 37 °C for 6~8 h in the conditioned media containing various concentrations (0, 0.78, 1.56, 3.13, and 6.25 μM) of CyH. The tube formation in A549 (A) and H460 (B) was observed under a phase-contrast microscope (original magnification, ×200). The total tube length in three random view-fields per well was measured by Scion Image software, and average value was calculated. The results represented the mean ± SD from three replicate experiments. Compared with control (lane 2), **$P < 0.01$.
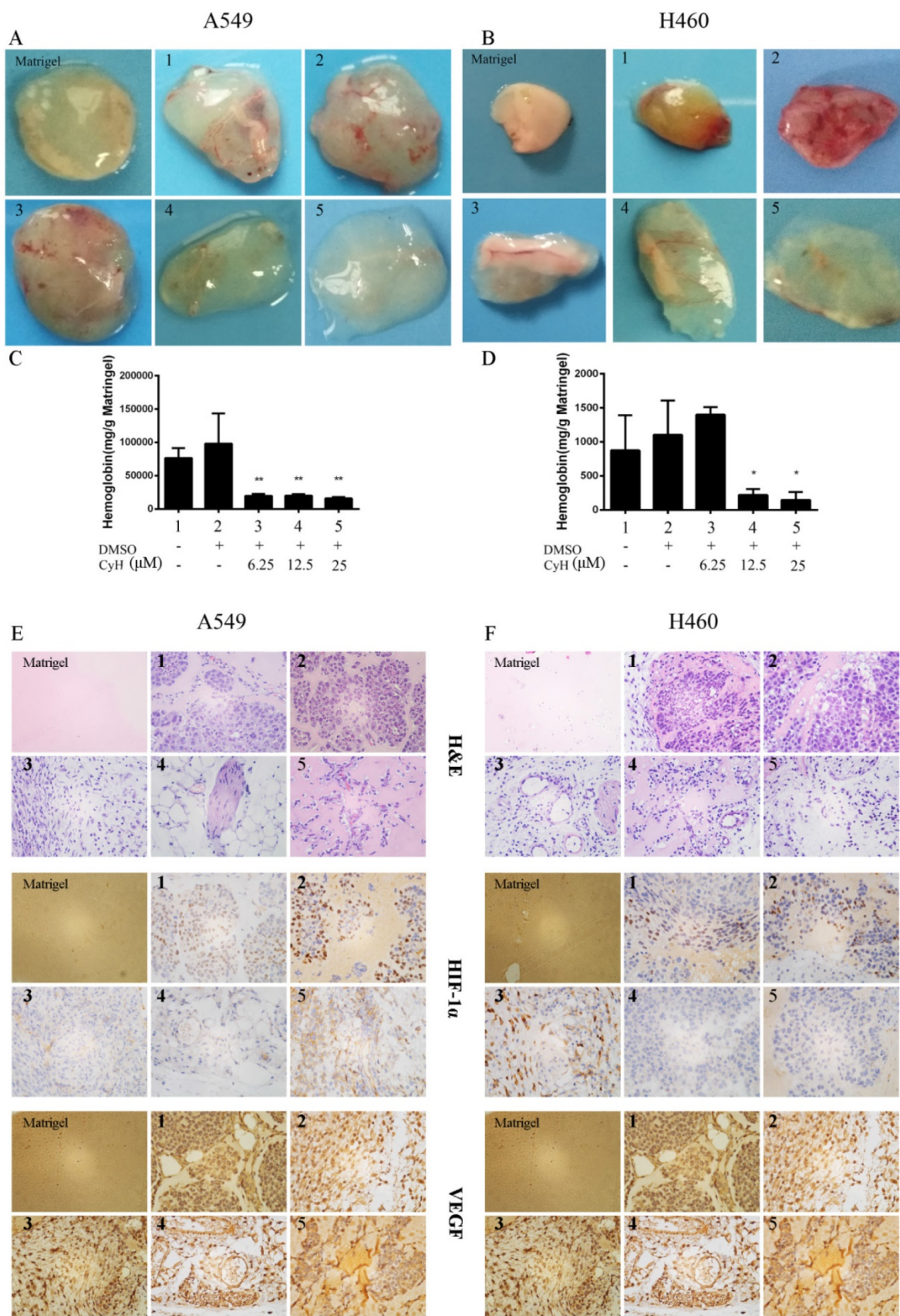
Figure 2. CyH inhibited angiogenesis *in vivo* and HIF-1α and VEGF protein expression in A549 and H460 NSCLC xenografts. A549 and H460 cells were treated with different concentrations (0, 6.25, 12.5, and 25 μM) of CyH. (A, B) Matrigel plugs. (C, D) The hemoglobin levels in Matrigel plugs. Hemoglobin content was expressed as (mg/g) of Matrigel plug. Immunohistochemical studies on the expression of HIF-1α (F) and VEGF (G) proteins in A549 and H460 xenografted tumors (original magnification, ×400). The results are representative of five independent experiments. Compared with control (lane 2),*P<0.05, **P<0.01.
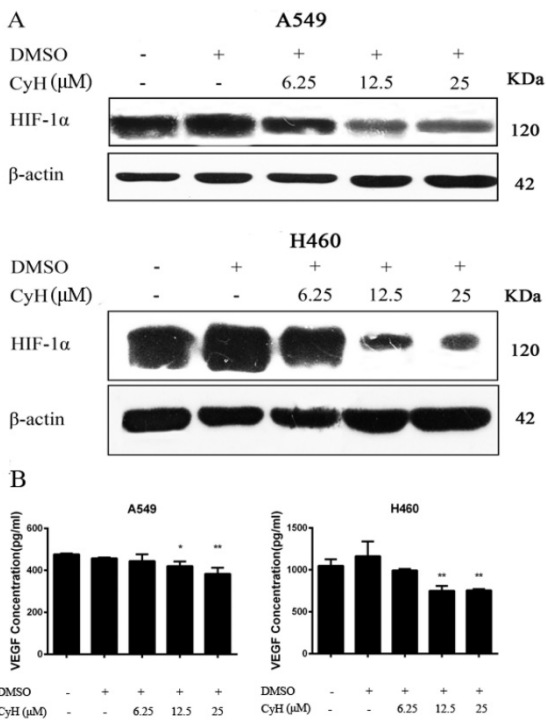
Figure 3. CyH inhibited HIF-1α and VEGF protein expression in A549 and H460 cells. A549 and H460 cells were treated with different concentrations (0, 6.25, 12.5, and 25 μM) of CyH for 24 h. (A) Western blot analysis was performed to detect the expression of HIF-1α protein. (B) VEGF protein production in the conditioned media was determined by ELISA. Results are representative of three independent experiments. Compared with control (lane 2),*P<0.05, **P<0.01.
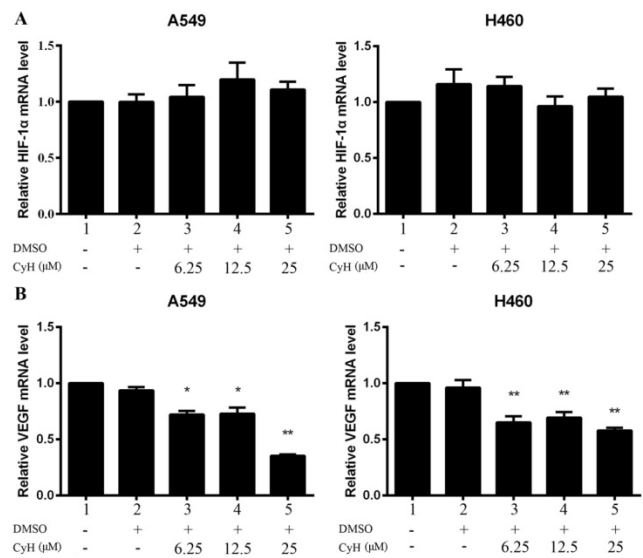

Figure 5. Effects of CyH on the degradation of HIF-1α protein in A549 and H460 cells. A549 (A) and H460 (B) cells were pre-treated with cycloheximide (CHX; 10 μg/mL) for different time periods, followed by the treatment with 6.25 μM of CyH for 24 h. HIF-1α protein expression was determined by Western blot analysis. The results were representative of three independent experiments.

Figure 4. Effect of CyH on HIF-1α and VEGF mRNA expression in A549 and H460 cells. A549 and H460 cells were treated with different concentrations (0, 6.25, 12.5, and 25 μM) of CyH for 24 h. RT-qPCR was performed to determine HIF-1α (A) and VEGF (B) mRNA levels. The relative value of the control (lane 1) was arbitrarily set as 1.0. The results represented the mean ± SD from three replicate experiments. Compared with control (lane 2), *P<0.05, **P<0.01.

CyH inhibited HIF-1α protein accumulation and VEGF expression in A549 and H460 cells

In A549 and H460 cells, we also found that CyH inhibited HIF-1α protein expression **(Figure 3A)**. At the same time, CyH at 12.5 and 25 μM significantly inhibited the secretion of VEGF protein in A549 and H460 cells in a concentration-dependent manner ($P<0.01$, **Figure 3B**). To study whether the suppression of HIF-1α and VEGF protein expression was the result of transcriptional inhibition, HIF-1α and VEGF mRNA levels were determined by RT-qPCR. As shown in **Figure 4**, CyH had a significantly inhibitory effect on the expression of VEGF mRNA (P<0.05), but had no obvious effect on HIF-1α mRNA expression in A549 and H460 cells, suggesting that CyH inhibited HIF-1α protein expression through a posttranscriptional mechanism.

CyH inhibited HIF-1α protein expression by promoting its degradation in A549 and H460 cells

RT-qPCR analysis showed that CyH did not significantly affect HIF-1α mRNA level **(Figure 4A)**, while CyH downregulated HIF-1α protein expression in A549 and H460 cells **(Figure 2)**. To explore whether CyH treatment affects the stability of HIF-1α protein, cycloheximide (CHX), a protein translation inhibitor, was utilized to prevent *de novo* HIF-1α protein synthesis in the presence or absence of CyH. The stability of HIF-1α protein was reduced in CyH-treated A549 and H460 cells in comparison with
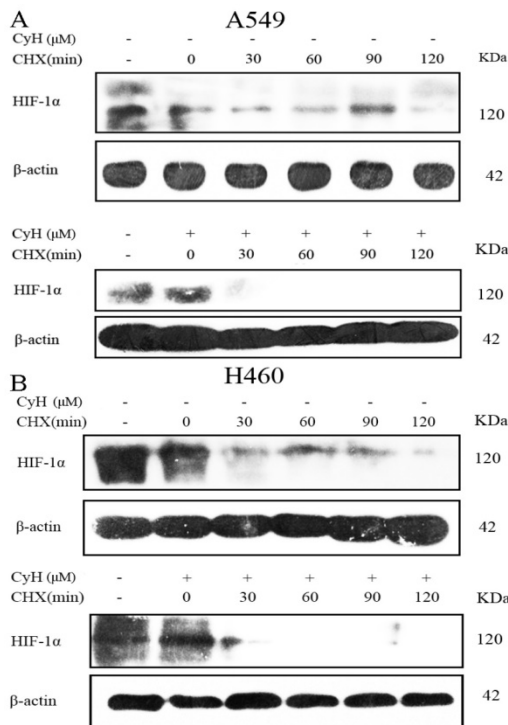
controls **(Figure 5).** The half life of HIF-1α protein in CyH-treated cells (A549: 13.88±1.12 min, H460: 21.12±2.43 min) was much shorter than that in control cells (A549: 57.893±11.83 min, H460: 66.22±12.42 min), indicating that CyH accelerated the degradation of HIF-1α protein. Collectively, our findings suggested that CyH decreased HIF-1α protein levels mainly by promoting its degradation.

CyH inhibited angiogenesis through the suppression of PI3K/AKT/P70S6K and ERK1/2 pathways in A549 and H460 cells

To determine whether CyH inhibits tumor angiogenesis by suppressing PI3K/AKT/P70S6K and ERK1/2 signaling pathways, we detected the phosphorylation of AKT, P70S6K, and ERK1/2 by western blot analysis. As showed in **Figure 6**, the expressions of p-AKT, p-P70S6K, and p-ERK1/2 were inhibited in CyH-treated A549 and H460 cells, and the inhibitory effects were also enhanced with the increase of CyH concentration.

Discussion

Lung cancer, as the primary cause of cancer death worldwide, is the most commonly diagnosed cancer worldwide. Current chemotherapeutic approaches show serious undesirable side effects as well as intrinsic or acquired chemoresistance in patients [1, 31, 32]. Therefore, it is urgent to search for

new anticancer drugs with advanced efficiency and fewer side effects [33].

In our previous studies, we isolated CyH from the mangrove-derived endophytic fungus *Phomopsis* sp. in Zhanjiang, China, and demonstrated that CyH induced apoptosis and inhibited migration with low toxicity in A549 NSCLC cells [25]. Moreover, Lee *et al* [26] found that CyH extracted from *G. sinensis* thorns is an active anti-angiogenic constituent. Angiogenesis is a key mediator of NSCLC progression, and anti-angiogenic therapy has been proven to be beneficial to patients with NSCLC [34, 35]. Therefore, we investigated whether CyH was useful in the prevention and treatment for NSCLC. In this study, we demonstrated that CyH dramatically inhibited NSCLC angiogenesis both *in vitro* (**Figure 1**) and *in vivo* (**Figure 2**), suggesting that CyH may be a potential agent for the prevention and treatment of NSCLC.

HIF-1α, activated by hypoxic stress, plays an important role in promoting cancer angiogenesis [36]. HIF-1α activates transcription of the promoter of VEGF, an important factor in angiogenesis and invasion [37]. In the present study, we found that CyH inhibited HIF-1α protein accumulation and VEGF expression in A549 and H460 NSCLC cells **(Figure 3 and 4)**. Meanwhile, immunohistochemical results further confirmed that CyH obviously inhibited HIF-1α and VEGF expression in the NSCLC xenografts of nude mice **(Figure 2E and 2F)**. These results suggest that HIF-1α and VEGF may be key molecular targets for CyH against angiogenesis of NSCLC.

In this study, we demonstrated that CyH had no effect on HIF-1α mRNA expression in A549 and H460 cells, implying the involvement of posttranscriptional mechanism. Moreover, our results further showed that CyH inhibited HIF-1α protein expression by accelerating the degradation of HIF-1α protein **(Figure 5)**. HIF-1α can directly interact with the von Hippel–Lindau (VHL), triggering the ubiquitination and subsequent degradation *via* the 26S proteasome system [38, 39]. It suggested that CyH suppressed HIF-1α protein accumulation in A549 and H460 cells mainly by promoting its degradation *via* the 26S proteasome system, which needs to be further studied.

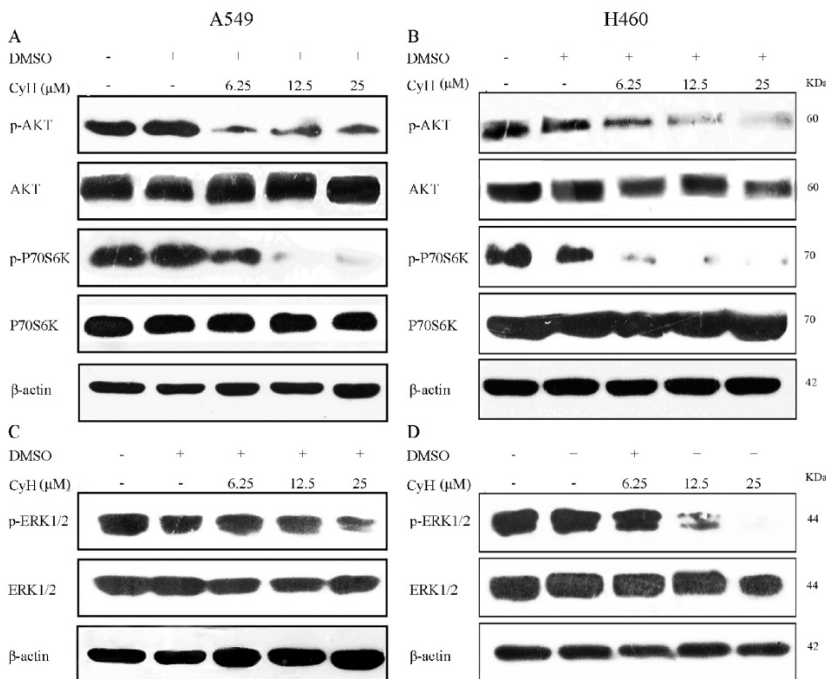PI3K/AKT/mTOR and ERK1/2 signaling pathways regulate the

Figure 6. Effect of CyH on activation of PI3K/AKT/P70S6K and ERK1/2 signaling pathways. A549 and H460 cells were treated with different concentrations (0, 6.25, 12.5, and 25 μM) of CyH for 24 h. Protein samples (100 μg) were subjected to 10% SDS-PAGE, and phosphorylated ERK, AKT, and P70S6K protein expression was detected by Western blot analysis.

growth, survival, migration, and epithelial-mesenchymal transition in cancer cells [40–43]. AKT stimulates angiogenesis by increasing cell migration and invasion [44]. A growing body of evidence demonstrates that P70S6K can regulate angiogenesis [45]. Therefore, to further understand the signaling mechanisms by which CyH inhibited HIF-1α protein accumulation, we next examined the effects of CyH on the activation of PI3K/AKT/ P70S6K and ERK1/2 pathways in A549 and H460 cells. Our results showed that CyH significantly inhibited AKT, P70S6K, and ERK1/2 activation in A549 and H460 cells **(Figure 6)**, which was consistent with its inhibitory effects on HIF-1α and VEGF protein expression **(Figure 3)**. Taken together, these results indicate that CyH inhibits PI3K/AKT/P70S6K and ERK1/2 signaling pathways to suppress HIF-1α protein expression in A549 and H460 cells.

In conclusion, in this study, we demonstrated for the first time, to the best of our knowledge, that CyH inhibited NSCLC angiogenesis *in vitro* and *in vivo*, which may be involved in the inhibition of HIF-1α protein accumulation and VEGF expression *via* PI3K/AKT/P70S6K and ERK1/2 signaling pathways. These findings suggest that CyH may be developed into a potential drug for anti-angiogenesis of NSCLC.

Acknowledgments

Competing Interests

The authors have declared that no competing interest exists.

References

1. Chen W, Zheng R, Baade PD, et al. Cancer statistics in China, 2015. CA Cancer J Clin. 2016; 66: 115-32.
2. Torre LA, Siegel RL, Jemal A. Lung Cancer Statistics. Adv Exp Med Biol. 2016; 893: 1-19.
3. Siegel RL, Miller KD, Jemal A. Cancer statistics, 2016. CA Cancer J Clin. 2016; 66: 7-30.
4. Bray F, Ferlay J, Soerjomataram I, et al. Global cancer statistics 2018: GLOBOCAN estimates of incidence and mortality worldwide for 36 cancers in 185 countries. CA Cancer J Clin. 2018; 68(6): 394-424.
5. Reck M, Heigener DF, Mok T, et al. Management of non-small-cell lung cancer: recent developments. Lancet. 2013; 382: 709-19.
6. DeSantis CE, Lin CC, Mariotto AB , et al. Cancer treatment and survivorship statistics, 2014. CA Cancer J Clin. 2014; 64: 252-71.
7. Minguet J, Smith KH, Bramlage P. Targeted therapies for treatment of non-small cell lung cancer--Recent advances and future perspectives. Int J Cancer. 2016; 138: 2549-61.
8. Chansky K, Subotic D, Foster NR, et al. Survival analyses in lung cancer. J Thorac Dis. 2016; 8: 3457-63.
9. Cho H, Mariotto AB, Schwartz LM, et al. When do changes in cancer survival mean progress? The insight from population incidence and mortality. J Natl Cancer Inst Monogr. 2014; 2014: 187-97.
10. Hanahan D, Weinberg RA. Hallmarks of cancer: the next generation. Cell. 2011; 144: 646-74.
11. Cristi E, Perrone G, Toscano G, et al. Tumour proliferation, angiogenesis, and ploidy status in human colon cancer. J Clin Pathol. 2005; 58: 1170-74.
12. Kanno S, Oda N, Abe M, et al. Roles of two VEGF receptors, Flt-1 and KDR, in the signal transduction of VEGF effects in human vascular endothelial cells. Oncogene. 2000; 19: 2138-46.
13. Meadows KN, Bryant P, Vincent PA, et al. Activated Ras induces a proangiogenic phenotype in primary endothelial cells. Oncogene. 2004; 23:192-200.
14. Bai X, Cerimele F, Ushio-Fukai M, et al. Honokiol, a small molecular weight natural product, inhibits angiogenesis in vitro and tumor growth in vivo. J Biol Chem. 2003; 278: 35501-7.
15. Qian J, Bai H, Gao Z, et al. Downregulation of HIF-1α inhibits the proliferation and invasion of non-small cell lung cancer NCI-H157 cells. Oncol Lett. 2016; 11: 1738-44.
16. Zhong H, De Marzo AM, Laughner E, et al. Overexpression of hypoxia-inducible factor 1alpha in common human cancers and their metastases. Cancer Res. 1999; 59: 5830-5.
17. Ferrar N, Gerber HP, LeCouter J. The biology of VEGF and its receptors. Nat Med. 2003; 9: 669-76.
18. Park JJ, Hwang SJ, Park JH, et al. Chlorogenic acid inhibits hypoxia-induced angiogenesis via down-regulation of the HIF-1α/AKT pathway. Cell Oncol (Dordr). 2015; 38: 111-8.
19. Mineo TC, Ambrogi V, Baldi A, et al. Prognostic impact of VEGF, CD31, CD34, and CD105 expression and tumour vessel invasion after radical surgery for IB-IIA non-small cell lung cancer. J Clin Pathol. 2004; 57: 591-7.
20. Abu-Jawdeh GM, Faix JD, Niloff J, et al. Strong expression of vascular permeability factor (vascular endothelial growth factor) and its receptors in ovarian borderline and malignant neoplasms. Lab Invest. 1996; 74: 1105-15.
21. Ferrara N, Gerber HP, LeCouter J. The biology of VEGF and its receptors. Nat Med. 2003; 9: 669-76.
22. Cooney MM, van Heeckeren W, Bhakta S, et al. Drug insight: vascular disrupting agents and angiogenesis--novel approaches for drug delivery. Nat Clin Pract Oncol. 2006; 3: 682-92.
23. Sharma R, Khaket TP, Dutta C, et al. Breast cancer metastasis: Putative therapeutic role of vascular cell adhesion molecule-1. Cell Oncol (Dordr). 2017; 40: 199-208.
24. Wu JB, Tang YL, Liang XH. Targeting VEGF pathway to normalize the vasculature: an emerging insight in cancer therapy. Onco Targets Ther. 2018; 11: 6901-9.
25. Ma Y, Wu X, Xiu Z, et al. Cytochalasin H isolated from mangrovederived endophytic fungus induces apoptosis and inhibits migration in lung cancer cells. Oncol Rep. 2018; 39: 2899-905.
26. Lee J, Yi JM, Kim H, et al. Cytochalasin H, an active anti-angiogenic constituent of the ethanol extract of Gleditsia sinensis thorns. Biol Pharm Bull. 2014; 37: 6-12.
27. Udagawa T, Yuan J, Panigrahy D, et al. Cytochalasin E, an epoxide containing Aspergillus-derived fungal metabolite, inhibits angiogenesis and tumor growth. J Pharmacol Exp Ther. 2000; 294: 421-7.
28. Zhang E, Feng X, Liu F, et al. Roles of PI3K/Akt and c-Jun signaling pathways in human papillomavirus type 16 oncoprotein-induced HIF-1α, VEGF, and IL-8 expression and in vitro angiogenesis in non-small cell lung cancer cells. PLoS One. 2014; 9: e103440.
29. Li G, He L, Zhang E, et al. Overexpression of human papillomavirus (HPV) type 16 oncoproteins promotes angiogenesis via enhancing HIF-1α and VEGF expression in non-small cell lung cancer cells. Cancer Lett. 2011; 311: 160-70.
30. He L, Zhang E, Shi J, et al. (-)-Epigallocatechin-3-gallate inhibits human papillomavirus (HPV)-16 oncoprotein-induced angiogenesis in non-small cell lung cancer cells by targeting HIF-1α. Cancer Chemother Pharmacol. 2013; 71: 713-25.
31. El-Aarag B, Kasai T, Masuda J, et al. Anticancer effects of novel thalidomide analogs in A549 cells through inhibition of vascular endothelial growth factor and matrix metalloproteinase-2. Biomed Pharmacother. 2017; 85: 549-555.
32. Chang L, Gong F, Cai H, et al. Combined RNAi targeting human Stat3 and ADAM9 as gene therapy for non-small cell lung cancer. Oncol Lett. 2016; 11: 1242-50.
33. Nishanth Kumar S, Aravind SR, Jacob J, et al. Pseudopyronine B: A Potent Antimicrobial and Anticancer Molecule Isolated from a Pseudomonas mosselii. Front Microbiol. 2016; 7: 1307.
34. Das M, Wakelee H. Targeting VEGF in lung cancer. Expert Opin Ther Targets. 2012; 16: 395-406.
35. Shojaei F. Anti-angiogenesis therapy in cancer: current challenges and future perspectives. Cancer Lett. 2012; 320: 130-7.

36. Jung DB, Lee HJ, Jeong SJ, et al. Rhapontigenin inhibited hypoxia inducible factor 1 alpha accumulation and angiogenesis in hypoxic PC-3 prostate cancer cells. Biol Pharm Bull. 2011; 34: 850-5.

37. Xie Y, Qi Y, Zhang Y, et al. Regulation of angiogenic factors by the PI3K/Akt pathway in A549 lung cancer cells under hypoxic conditions. Oncol Lett. 2017; 13: 2909-14.

38. Kaelin WJ. The von Hippel-Lindau tumour suppressor protein: O2 sensing and cancer. Nat Rev Cancer. 2008; 8: 865-73.

39. Ji Q, Burk RD. Downregulation of integrins by von Hippel-Lindau (VHL) tumor suppressor protein is independent of VHL-directed hypoxia-inducible factor alpha degradation. Biochem Cell Biol. 2008; 86: 227-34.

40. Gates MA, Tworoger SS, Hecht JL, et al. A prospective study of dietary flavonoid intake and incidence of epithelial ovarian cancer. Int J Cancer. 2007; 121: 2225-32.

41. Karar J, Maity A. PI3K/AKT/mTOR Pathway in Angiogenesis. Front Mol Neurosci. 2011; 4: 51.

42. Zheng HL, Wang LH, Sun BS, et al. Oligomer procyanidins (F2) repress HIF-1alpha expression in human U87 glioma cells by inhibiting the EGFR/AKT/mTOR and MAPK/ERK1/2 signaling pathways in vitro and in vivo. Oncotarget. 2017; 8: 85252-62.

43. Liu J, Huang B, Xiu Z, et al. PI3K/Akt/HIF-1alpha signaling pathway mediates HPV-16 oncoprotein-induced expression of EMT-related transcription factors in non-small cell lung cancer cells. J Cancer. 2018; 9(19): 3456-66.

44. Aksamitiene EA, Kiyatkin, Kholodenko BN. Cross-talk between mitogenic Ras/MAPK and survival PI3K/Akt pathways: a fine balance. Biochem Soc Trans. 2012; 40: 139-46.

45. Saraswati S, Kumar S, Alhaider AA. α-santalol inhibits the angiogenesis and growth of human prostate tumor growth by targeting vascular endothelial growth factor receptor 2-mediated AKT/mTOR/P70S6K signaling pathway. Mol Cancer. 2013; 12: 147.